INVESTIGATION ON DRAG REDUCTION PHENOMENON IN OIL-WATER DISPERSED PIPE FLOW VIA WIRE-MESH SENSOR

Rodriguez, I. H., iarahr@sc.usp.br
Yamaguti, H. K. B., henrique_kazuo@yahoo.com.br
de Castro, M.S., marscastro@gmail.com
Nucleo de Engenharia Térmica e Fluidos (NETeF)
Departamento de Engenharia Mecanica, Escola de Engenharia de Sao Carlos, Universidade de Sao Paulo (EESC-USP)
Av Trabalhador Sao Carlense, 400
13566-590 Sao Carlos- SP- Brazil

Da Silva, M. J., m.dasilva@fzd.de
Forschungszentrum Dresden-Rossendorf e. V., Institute of Safety Research, PO Box 510119, 01314, Dresden, Germany

Rodriguez, O. M. H., oscarmhr@sc.usp.br
Nucleo de Engenharia Térmica e Fluidos (NETeF)
Departamento de Engenharia Mecanica, Escola de Engenharia de Sao Carlos, Universidade de Sao Paulo (EESC-USP)
Av Trabalhador Sao Carlense, 400
13566-590 Sao Carlos- SP- Brazil

Abstract. *Liquid-liquid flows are present in a wide range of industrial processes; however they have not been studied as intensively as gas-liquid flows. The interest in two-phase liquid-liquid flows has increased recently mainly due to the petroleum industry where oil and water are often produced and transported together for long distances. Nevertheless, the frictional pressure gradient in oil-water pipe flow not rare cannot be predicted by correlations developed for gas-liquid flow. The dispersed flow pattern is common in crude oil transmission pipelines and offshore pipelines, with either oil or water as the dominant phase. An interesting feature of dispersed flow is that it can behave as a non-Newtonian fluid. There are several works on drag reduction in single and gas-liquid two-phase flows, but only few on liquid-liquid flow. Drag reduction phenomenon in oil-water flows without the addition of any drag reduction agent has been detected in previous works, but the physics behind the phenomenon is yet not well understood. This work's main goal is the experimental study of the drag reduction phenomenon in dispersed oil-water flow. Pressure gradients were measured during the flow of oil (860 kg/m3 density and 100 mPa. s viscosity) and water. The experimental work was performed in a 12-m-long 2.62-cm-i.d. horizontal glass pipe. A new wire-mesh sensor based on capacitance (permittivity) has been employed in this study. The sensor consists of two layers made of 8 steel wires each separated 1 mm from each other. It is able to discriminate fluids having different relative permittivity values in a multiphase flow and was used to measure local, transient and time-and-space averaged phase fraction distributions in the flow cross-section. A high-speed video camera and the Quick Closing Valves technique were used to compare and validate the signals of the wire-mesh sensor.*

Keywords: *Liquid-liquid flow, Drag reduction, Dispersed flow, Pressure gradient, Wire-mesh sensor*

1. INTRODUCTION

Multiphase Flows are common in several industrial processes, as in the petroleum industry where not rare oil and water are transported together. The proper design of a two-phase production well or pipeline depends on the accurate prediction of the frictional pressure gradient, which usually cannot be made by extrapolation of single-phase codes. This has been one of the main reasons behind the great interest in the study of oil-water flows observed in recent years. However, liquid-liquid flows have not been studied as intensively as gas-liquid flows. In addition, despite its very common occurrence in the industry, oil-water dispersed flows (where one phase is dispersed as droplets into a continuous phase) have not been explored to the same extent as separated flows, usually annular and stratified, or intermittent flow patterns as slug flow.

Pal (1993) made a literature review on the pipe flow of oil-water and investigated the behavior of dispersions in laminar and turbulent horizontal flows. He found that such dispersions exhibit a phenomenon known as drag reduction in turbulent regime. The effective viscosity values obtained in turbulent regime are smaller than the equivalent values in laminar regime. This indicates a relative decrease of the pressure gradient in turbulent regime. The intensity of the drag reduction depends on the physical properties of the oil and on the concentration of the dispersed phase.

A number of researchers have detected the drag reduction phenomenon in oil-water flows. Angeli and Hewitt (1998) measured pressure gradients in oil-water horizontal flow and found an evident drag reduction for high mixture velocities (2.6-3.0m /s) and low fractions of water, where the dispersed pattern prevails (being the oil the continuous phase).Experimental friction factors were measured in oil-water flows with either oil or water as continuous phases and also in single phase flow of water and oil. The two-phase friction factors were significantly smaller than the single-

phase ones when the oil is the continuous phase and almost the same when the water is the continuous phase. Lovick and Angeli (2004) also observed a decrease in the two-phase pressure gradients with respect to equivalent single-phase values in oil-water horizontal dispersed flow. Rodriguez (2005) detected the same behavior observed by the previous authors in slightly-inclined oil-water flow, but, for the first time, it was verified that the phenomenon is a function of pipe inclination, the effect being increased in downward and reduced in upward inclinations. Ioannou et al. (2005) investigated the phase inversion and its effect in the pressure gradient in oil-water dispersed flow. They found a reduction in pressure gradient at low and high oil fraction compared to single phase water and oil values, respectively, for all velocities studied. Lum *et al.* (2006) studied the effect of pipe inclination on the flow pattern, pressure gradient and holdup in oil-water flow. A reduction of pressure gradient was observed until a minimum that was reached between 60 and 80% of oil for high mixture velocities. The frictional pressure gradient in upward and downward flows was in general lower than in horizontal flows while the minimum occurred at all inclinations at high mixture velocities. Hu and Angeli (2006) investigated experimentally the phase inversion phenomenon in a vertical steel pipe (co-current upward and downward flows). They observed a reduction in pressure gradient from the equivalent single phase oil and water values with the addition of small fractions of water or oil, respectively. Pal (2007) proposed a new mechanism for the modeling of drag reduction phenomenon in turbulent oil in water and water in oil dispersions. In this work was observed that oil-water emulsions and dispersions show drag reduction in turbulent flow. The measured friction factors in turbulent flow fall below the values expected on the basis of laminar flow. Based on the mixture effective rheological aspects, the phenomenon in oil-water dispersions is caused by a significant reduction of the effective viscosity of the dispersion when the flow regime passes from laminar to turbulent. It was observed that the degree of reduction is higher when the oil is the continuous phase.

It is interesting to note that the drag reduction phenomenon in oil-water dispersed flows has been detected by some researchers, but the physics and the mechanism behind the phenomenon is yet not well understood. The main goals of this work are the investigation of the two-phase drag reduction phenomenon in order to better understand it and the obtaining of new experimental data in oil-water dispersed flows therefore supplementing the information available in the literature. The wire-mesh sensor was applied for the first time for investigating flows involving viscous oil and water.

2. EXPERIMENTAL WORK

2.1 Test Facility

The experiments were performed in the Multiphase-Flow-loop Test Facility of NETeF (Thermal-Fluids Engineering Laboratory) of the Engineering School of São Carlos. The facility consists basically of a flow loop with the following component: pumps, test section, flow meters, differential transducer, compressor, separators and storage tanks. The flow Loop is represented in Fig. 1. Oil (860 kg/m^3 density and 100 mPa s viscosity) and water were investigated in a 2.62-cm-i.d. 12-m-long horizontal glass pipe. Both water and oil are kept in separated storage tanks. Each liquid is injected from the respective tanks to a mixer and then the test section through its own line and pump (positive displacement screw pumps). After the test section the mixture flows to a coalescent-plate separator tank. The phases once separated are returned to their respective storage tanks by gravity. Pressure-gradient data for oil-water two-phase flow and single-phase water flow at the same mixture velocity were collected. It was used a previously calibrated differential pressure transducer (SMAR LD301D). The pressure taps were located at 2.8 m and 8.9 m from the test section inlet, respectively.

The flow patterns were identified by means of two different techniques. A high speed video camera (Optronis, Camrecord 600) was used and allowed for a lateral view of the flow. The flow was recorded through a specially designed Perspex visualization section located at 10.3 m from the tube entrance. The recording speed was 2000 frames per second. A new wire-mesh sensor based in capacitance measurements (Da silva, 2007) was also used for the characterization of the flow patterns, since it offers a tomography of the cross-section of the flow. The wire-mesh sensor was installed at the end to the horizontal test section, to 10.3 m from the tube entrance. To assemble the wire-mesh sensor in the test line a flange made entirely of transparent Perspex was manufactured in the NETeF (Fig. 2).

In-situ volume fraction (holdup) was measured via the quick-closing-valves technique (QCV). After reaching steady state, two remotely controlled pneumatic valves, placed at the ends of the pipe, and a third valve, connected to a by-pass line, were used to trap the mixture. The experimental uncertainty of the oil volume fraction measured by the QCV is estimated to be ranged from $\pm 0.88\%$ to $\pm 2.58\%$ (de Castro *et al.*, 2009). The holdup data was used to calibrate the wire-mesh sensor.

A computer was used to conduct the tests and collect the data. The input water and oil flow rates were setup via PXI National Instruments™ and Lab View™ program and measured through flowmeters, respectively: Vortex SMART Ex Delta VXW1050-N51L-1014A (high water flow rate), Positive Displacement OVAL OG (low water flow rate) and Positive Displacement OVAL LS5576-43-0A Type (oil flow rate).

The aim was to obtain a set of points of oil-water dispersed flow data that would cover the entire range of occurrence of the drag reduction phenomenon. The criterion used to determine the occurrence of the phenomenon was the ratio of two-phase flow pressure gradient and single-phase water flow pressure gradient at mixture flow rate. 64 points were

collected (a point means a pair of oil and water superficial velocities) and for each point the mixture and single-phase water pressure gradients were measured. Oil superficial velocity ranged from 0.2 m/s to 1.9 m/s and water superficial velocity ranged from 0.6 m/s to 3.0 m/s. The range of mixture velocities covered was $0.9 < J_m < 4$ m/s and the range of oil volume fraction was 10% to 70%.

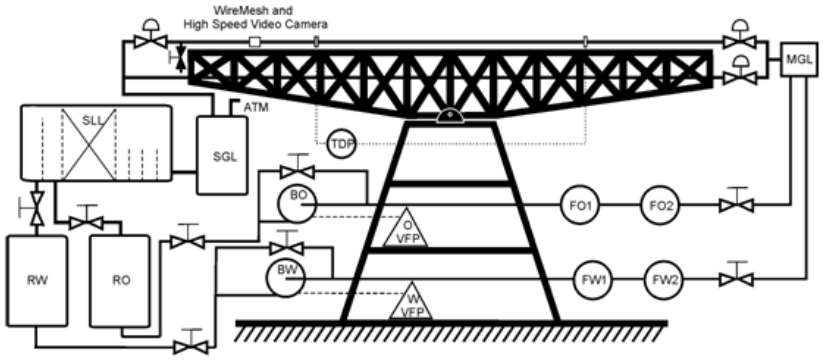

	W VFP – Water Variable-frequency driver O VFP – Oil Variable-frequency driver		FO1 – Oil High Flow Meter FO2 – Oil Low Flow Meter FW1 – Water High Flow Meter FW2 – Water Low Flow Meter
	Quick Closing Valve		Control Valve
TDP	Differential Pressure Transducer		BW – Water Pump BO – Oil Pump
SLL	Coalescent-plates liquid-liquid separator		Drainage Valve
MGL	Multiphase mixer	RW	Water Tank
RO	Oil Tank	SGL	Gas-liquid separator Tank

Figure 1. Schematic diagram of the two-phase flow loop and installation.

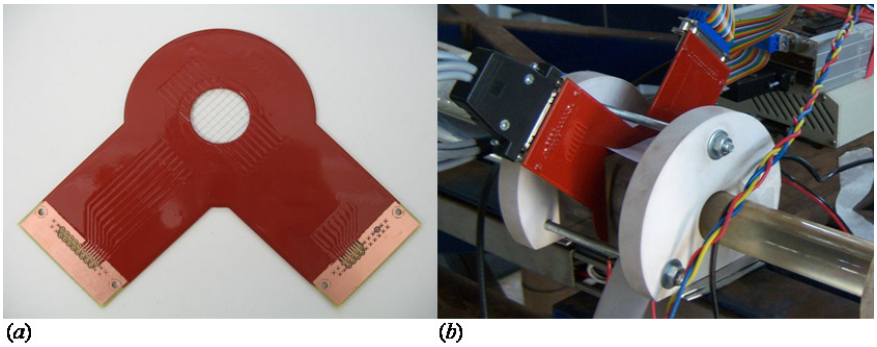

(*a*) (*b*)

Figure 2. (a) Photo of the wire-mesh sensor employed in this study; (b) part of the test section with integrated sensor.

2.2 Wire-Mesh Sensor

The wire-mesh sensor is a flow imaging device which allows the investigation of multiphase flow with high spatial and temporal resolution. First generation of this sensor was introduced about ten years ago by Prasser et al. (1998) and is based on conductivity measurements. In this work it was applied a novel wire-mesh sensor based on permittivity (capacitance) measurements which allows for investigating flows involving non-conducting fluids such as oil-air flows or oil-dominant oil-water flow.

The wire-mesh sensor is a hybrid in between intrusive local measurement of phase fraction and tomographic cross-sectional imaging. From the two-dimensional holdup distribution is possible to determine liquid holdup integrated over different domains thus obtaining time and/or spatially averaged holdup values, e.g. radial profiles or mean holdup (Da Silva, 2007).

The prototype sensor used in this work consists of two layers of 8 steel wires (0.12 mm diameter). The layers are separated 1 mm from each other. Within each plane the wires are evenly separated, i.e. 3 mm wire separation, which also determines the spatial resolution of the instrument. The sensor measures the permittivity of each crossing point of the grid formed by the wires in a fast manner. The transmitter wires are consecutively activated by means of a

sinusoidal excitation voltage, while the currents flowing towards the receiver wires are sampled in parallel. The non-activated transmitter wires are grounded. This assures that the electrical field is concentrated around a given crossing point, so that the measured currents are unambiguously related to the corresponding crossing point. In this way, the wire-mesh sensor subdivides the cross section in a number of sub-regions and determines the phase present in each one of those sub-regions independently in a fast and multiplexed way. Time resolution of the prototype sensor is 500 frames per second. The capacitance wire-mesh sensor principle is described in detail in Da Silva (2007).

The measured voltage of a wire-mesh sensor is proportional to the permittivity of the fluid surrounding a crossing point, k_x, according to Da Silva (2007)

$$V_{log}(i,j) = a(i,j)\,ln[k_x(i,j)] + b(i,j) \tag{1}$$

where the indices $i \in (1\ldots8)$ and $j \in (1\ldots8)$ represent crossing point positions in the cross section and the constants a and b are parameters related to the electronics (e.g. amplifier characteristics) which can be determined through a calibration routine as follows.

For calculating the constants a and b we need to measure the voltage of two substances with known permittivity. First, the voltage is measured with a substance of low permittivity (oil) covering the entire cross section of the sensor giving a reference value and the procedure is repeated with the substance of high permittivity (water), which gives another reference value. In this fashion, applying the Eq. (1) for both calibration values it is possible to calculate the constants a and b.

Finally, the permittivity over the cross-section can be determined by inverting the Eq. (1) and using the previously determined constants, thus

$$k_{(i,j,t)} = exp\left[\frac{V_{log}(i,j,t) - b(i,j)}{a(i,j)}\right] \tag{2}$$

where t is the temporal sampling point index. For the determination of the *in-situ* volume fraction (liquid holdup), a following relationship between the measured permittivity and holdup is used:

$$\varepsilon_{o,WMS} = \frac{k_o(k_w - k_m)}{k_m(k_w - k_o)} \tag{3}$$

where, k_o, k_w and k_m are the permittivity of oil, water and the mixture, respectively, and $\varepsilon_{o,WMS}$ is the oil holdup. This equation describes the series model of mixture permittivity (McKeen and Pugsley, 2002). It was found that this model better describes the behavior of dispersed liquid-liquid systems (see section 3.2.2). The electronics and the prototype used in the experiment work carried out in the NETeF were designed and manufactured in Dresden-Rossendorf Research Center (Germany).

2.3 Two-phase Friction Factor

The homogeneous model was applied for the modeling of the liquid-liquid dispersed flow and determination of the two-phase friction factor. In such a model the mixture is treated as a "pseudo-fluid" with holdup-weighted physical properties, therefore the assumption of no-slip is assumed (Wallis, 1969). The density of the mixture is given by

$$\rho_m = \rho_o C_o + (1 - C_o)\rho_w \tag{4}$$

in which

$$C_o = \frac{U_{os}}{U_{ws} + U_{os}} \tag{5}$$

where C_o is the oil cut, ρ_w and ρ_o and U_{ws} and U_{os} are water and oil densities and superficial velocities, respectively. Notice that in the homogeneous no-slip model the oil cut is equal to the oil *in-situ* volumetric fraction or holdup.

The mixture friction factor was obtained via the homogeneous model by

$$f_m = \left(\frac{dp}{dx}\right)_m \frac{2D}{\rho_m U_m^2} \tag{6}$$

where $(dp/dx)_m$ is the mixture pressure gradient, U_m is the mixture velocity ($U_m = U_{ws} + U_{os}$) and D is the pipe's internal diameter. Single-phase water friction factor was calculated by:

$$f_w = \left(\frac{dp}{dx}\right)_w \frac{2D}{\rho_w V^2} \tag{7}$$

where $(dp/dx)_w$ stands for single-phase water pressure gradient and V is the mean velocity of the single phase water flow, and for each run:

$$V = U_m \tag{8}$$

2.4 Effective Mixture Viscosity

The mixture viscosity was obtained by the homogeneous model as proposed in Guet *et al.* (2006). The mixture frictional pressure gradient is given by Eq. (6). The parameters ρ_m and U_m are calculated as described in section 2.3. The mixture friction factor, f_m, is given by the Blasius' friction law: $f_m = 0.3164\, Re_m^{-0.25}$, where the Reynolds number of the mixture, Re_m, is defined by

$$Re_m = \frac{\rho_m U_m D}{\mu_m} \tag{9}$$

The mixture viscosity, μ_m, can be readily calculated as a function of the measured mixture pressure gradient:

$$\mu_m = 1596.41 \frac{D^5}{U_m^7 \rho_m^3} \left(\frac{dp}{dx}\right)_m^4 \tag{10}$$

3. RESULTS AND DISCUSSION

3.1. Experimental Detection of Drag Reduction Phenomenon

3.1.1 Pressure Gradient

The pressure gradient in oil-water horizontal flow was normalized with respect to the pressure gradient of water flowing alone in the pipe at the same mixture velocity, $(dp/dx)_m$ / $(dp/dx)_w$. Results are shown in Fig. 3 for water velocities of 1, 1.5, 2.0, 2.5 and 3.0 m/s where the normalized mixture pressure gradient is given as a function of the oil superficial velocity. At water superficial velocities ranging from 1 to 2.5 m/s the mixture pressure gradient was lower than that of single-phase water flow at the same mixture velocity, but at the highest water velocity (3m/s) the same behavior was not observed.

In general there was not a significant variation of the pressure gradient with oil superficial velocity. The detected reduction of the mixture pressure gradient with respect to the equivalent single-phase flow is known as two-phase drag reduction phenomenon, detected previously in some works (Angeli, 1998; Pal, 1993 and Rodriguez, 2005).

3.1.2 Mixture Friction Factor

The experimental mixture and single-phase water friction factors were plotted against the Reynolds Number of the mixture (Fig. 4). At the highest oil volume fraction (70%) the mixture friction factor was higher than that of the single-phase water flow (Fig. 4a). At 60% of oil fraction (Fig. 4b) one could observe a trend of crossing between the lines. Finally, at lower oil volume fractions, 20% and 40% (Figs. 4c and d), the single-phase water friction factor was higher than the mixture friction factor. These results suggest that in oil-in-water dispersed flow the drag reduction occurs at low oil fractions.

3.1.3 Effective mixture Viscosity

The calculated mixture viscosity was plotted against the water cut ($C_w = U_{ws} / U_m$) in Fig. 5. The mixture viscosity was found to be lower than the water viscosity (0.001 Pa.s) for water cuts higher than 50%. These results suggest once more that in the oil-in-water dispersed flow studied the drag reduction occurred at low oil fractions.

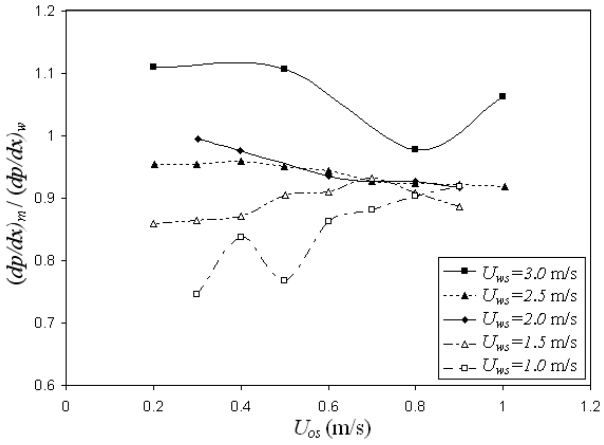

Figure 3. Normalized Pressure gradient against oil superficial velocity at different water superficial velocities.

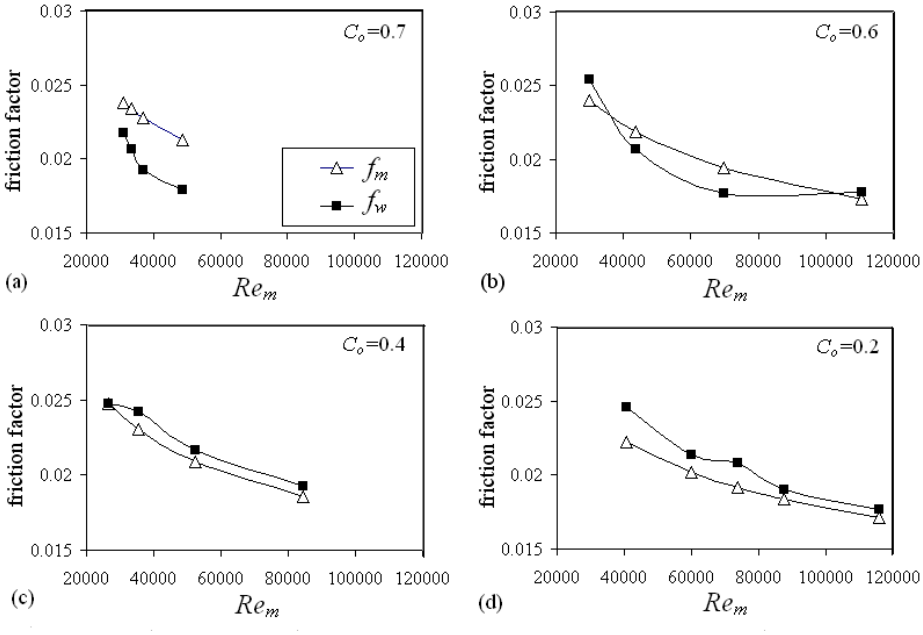

Figure 4. Mixture and single-phase water friction factors against mixture Reynolds number at different oil cuts.

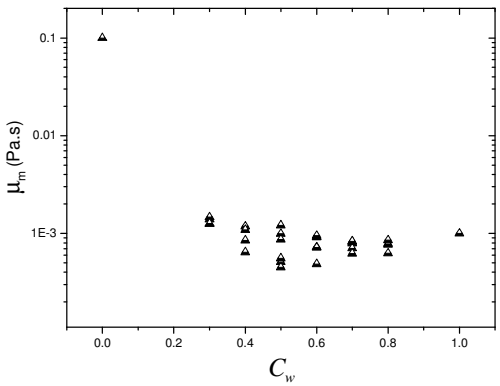

Figure 5. Mixture viscosity against the water cut.

3.2. Characterization of the Oil-water Flow

3.2.1 Flow patterns

High-speed video recording (2000 frames per second) was used to identify the flow patterns for the following flow conditions: oil velocity from 0.2 m/s to 1 m/s and water velocity from 1 m/s to 3m/s. At these flow conditions three different flow patterns were distinguished by watching the recorded movies in slow motion: Oil-in-water and Water-in-oil Dispersions (**Do/w & Dw/o**), Oil-in-water Homogeneous Dispersion **(o/w H)** and Oil-in-water Non-homogeneous Dispersion (**o/w NH**). Photographs of the flow patterns are shown in Fig. 5.

At the lowest tested water velocities (about 1 m/s) both phases were continuous and separated by an interface; however, both continuous phases entrained drops from each other (**Do/w & Dw/o**). When the water velocity was higher (about 1.5 m/s) a non-homogeneous dispersion of oil in water could be seen (**o/w NH**); in this case oil was dispersed as drops in the continuous water phase, but the drops had different sizes and were more concentrated at the top of the pipe. When the water velocity was even higher (about 2-3 m/s) a homogeneous dispersion of oil in water was observed (**o/w H**). In this case the dispersion of oil droplets was uniform.

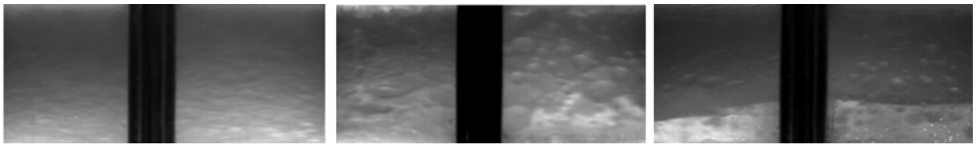

Figure 6. Pictures of the flow patterns observed in this work. (a) Oil-in-water Homogeneous Dispersion (**o/w H**), (b) Oil-in-water Non-Homogeneous Dispersion (**o/w NH**) and (c) Oil-in-water and Water-in-oil Dispersions (**Do/w & Dw/o**) (mixture flows from right to left and the wire-mesh sensor is seen as the black vertical stripe at the center).

3.2.2 Holdup

The oil holdup obtained via the quick-closing-valves technique (QCV) is compared with predictions of the homogeneous no-slip model. Then, it is also compared with the wire-mesh sensor measurements. The average relative error, *e*, is given by Eq. (9)

$$e = 100\frac{\sum N\sqrt{\left(\frac{\left(C_o, \varepsilon_{o,WMS}\right) - \varepsilon_{o,QCV}}{\varepsilon_{o,QCV}}\right)^2}}{N}[\%] \tag{11}$$

where subscript *WMS* and *QCV* stand for wire-mesh measurement and quick-closing-valves measurement, respectively. *N* is the number of experiments. The spreading of data is also an indicative of accuracy.

Figure 7 shows a comparison between the oil cut (Eq. 5) and the oil holdup experimentally obtained by the quick-closing-valves technique ($\varepsilon_{o,\ QCV}$). The dashed line indicates a deviation of 15 %. Quite surprisingly the homogeneous model overestimates the data, which indicates that oil is flowing faster than water. The overall relative error is 7.78 % and the accuracy is 15%.

In Fig. 8, the oil holdup measured via wire-mesh sensor is compared with the oil holdup measured via QCV. The relative error is 13.6%, whereas the accuracy is of 15%, which is considered a quite good result. Such performance provides valuable guidelines on the applicability of wire-mesh sensor in the investigation of two-phase flows involving viscous oil and water.

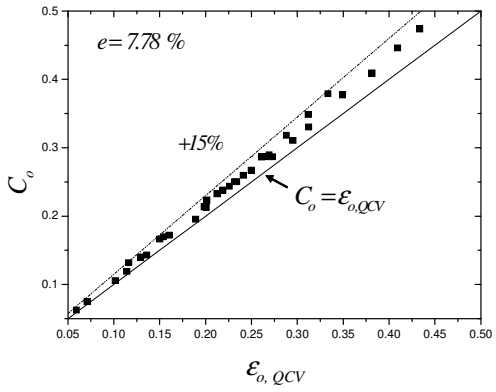

Figure 7. Oil cut predicted by the homogeneous model (C_o) against the oil holdup obtained via QCV ($\varepsilon_{o,\ QCV}$).

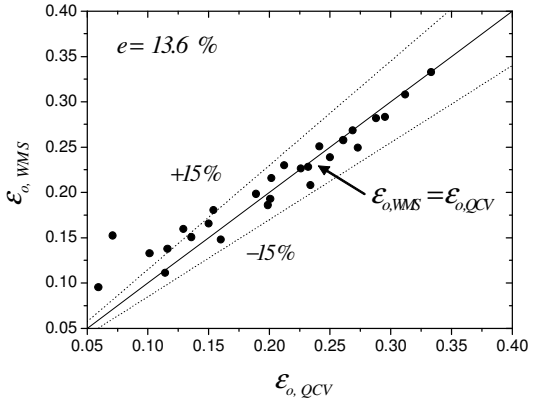

Figure 8. Oil Holdup measured via wire-mesh sensor ($\varepsilon_{o,\,WMS}$) against the oil holdup measured via QCV ($\varepsilon_{o,\,QCV}$).

3.2.3. Wire-mesh measurements

The two-dimensional local-instantaneous oil fraction distribution measured by the wire-mesh sensor can be used to determine oil fraction integrated over different domains, thus obtaining time and/or spatially averaged oil fraction values for all the experimental points. Figure 9 shows the results obtained via wire-mesh sensor for the three different flow patterns identified: **o/w H** (U_{ws}=*2.5 m/s,* U_{os}=*0.8 m/s*), **o/w NH** (U_{ws}=*1.5 m/s,* U_{os}=*0.8 m/s*) and **Do/w & Dw/o** (U_{ws}=*1.0 m/s,* U_{os}=*0.8 m/s*).

A time sampling of instantaneous space averaged oil fraction is showed in Fig. 9a. Average of the instantaneous space averaged fraction values provided the oil holdup, $\varepsilon_{o,WMS}$, which was compared with the holdup measured by the QCV. Figure 9b shows the frequency-domain representation of the holdup signal. In Fig. 9c, it is showed a radial oil fraction distribution, which is obtained by averaging the space averaged fraction in time. In fig. 9c, the space averaged local fraction is accomplished over a number of ring-shaped domains going from the center to the pipe wall over the cross section. Figures 9d and e show vertical and horizontal oil fraction distributions, which are obtained by averaging the space averaged local holdup in time. In Fig. 9d, the space averaged local fraction is accomplished over a number of vertical domains going from left to right over the cross section. In Fig. 9e, the space averaged local fraction is accomplished over a number of horizontal domains going from top to bottom over the cross section. Therefore, Fig. 9d offers the chordal oil holdup distribution from left to right and Fig. 9e offers the chordal holdup distribution from top to bottom of the pipe.

One can see in Fig. 9c that the decrease of oil holdup is intensified near to the pipe wall for the 3 different flow patterns. Even for the supposedly homogeneous **o/w H** it is observed a clear decrease in the oil fraction near to the wall. The significant reduction of the oil fraction for **o/w H** occurs at approximately 4 mm to the pipe wall. Figures 9d and e also confirm the existence of a higher amount of water near to the pipe wall for all flow patterns. Two quite interesting remarks should be drawn based on the results. The flow pattern where both continuous phases entrain drops from each other (**Do/w & Dw/o**) was not expected to present any fraction of water at the top of the pipe, but Fig. 9e clearly shows a decrease of oil holdup at the top of the pipe. On the other hand, the homogeneous dispersion of oil in water (**o/w H**), where the dispersion of oil droplets was supposed to be uniform over the cross section, also presents a clear decrease of oil holdup near to pipe wall (Figs. 9d and e).

Figure 10 shows space and time averaged oil holdup for each crossing point over the cross section for all three flow patterns. Figures 10a, b and c are related to the same experimental points described above, **o/w H** (U_{ws}=*2.5 m/s,* U_{os}=*0.8 m/s*), **o/w NH** (U_{ws}=*1.5 m/s,* U_{os}=*0.8 m/s*) and **Do/w & Dw/o** (U_{ws}=*1.0 m/s,* U_{os}=*0.8 m/s*), respectively. Data indicate that for **Do/w & Dw/o** the interface curves upwards (concave shape) and causes the water phase to have a higher wall contact area and the topmost layer seems to still have a significant fraction of water (Fig.10c). For **o/w NH** the same trend seems to be observed, but, as the holdup distribution is almost homogeneous, no interface can be observed. Once more, a significant water fraction can be seen at the top of the pipe. Finally, for **o/w H** the holdup distribution was practically uniform. Nevertheless, even in the homogeneously dispersed flow one may see an increase of the water fraction at the top of the pipe.

As a whole, results suggest that a water film may be surrounding the mixture of oil in water in all dispersed flow patterns observed in this work, which might be the physical mechanism behind the observed drag reduction phenomenon.

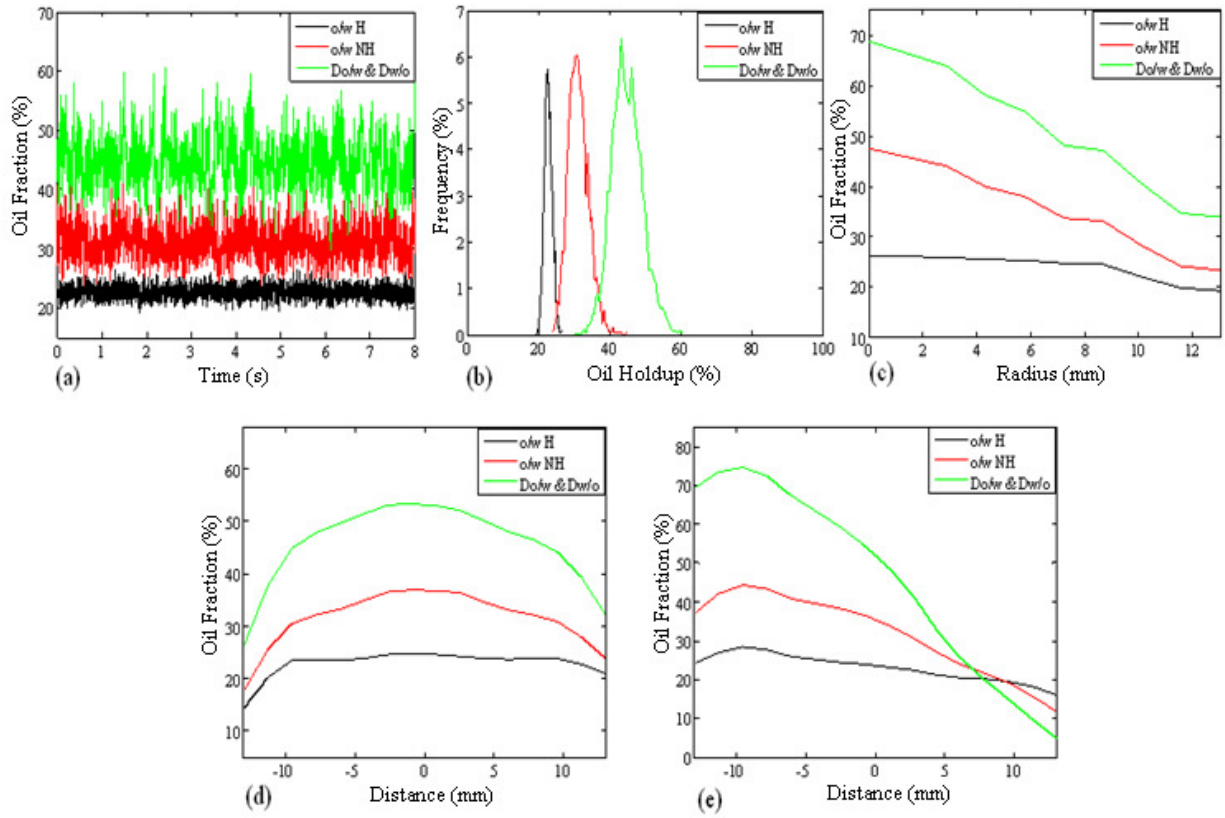

Figure 9. Wire-mesh sensor measurements for 3 different oil-water flow patterns, **o/w H**, **o/w NH** and **Do/w & Dw/o** (a) Time-domain holdup signal; (b) Frequency-domain holdup signal; (c) Time and ring-shaped domains radial profiles of oil fraction; (d) Chordal oil fraction distribution from left to right of the pipe; (e) Chordal oil fraction distribution from top to bottom of the pipe.

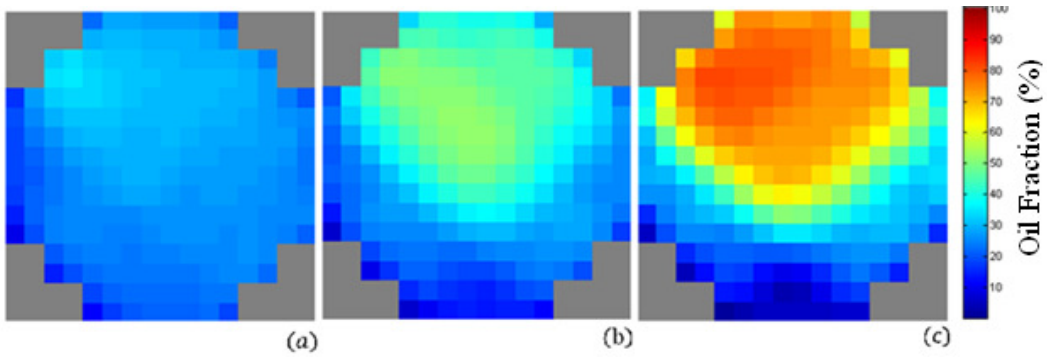

Figure 10. Cross-sectional images of phase distribution acquired with the capacitance wire-mesh sensor: (a) Oil-in-water Homogeneous Dispersion *(U_{ws}=2.5 m/s, U_{os}=0.8 m/s)*, (b) Oil-in-water Non-Homogeneous Dispersion *(U_{ws}=1.5 m/s, U_{os}=0.8 m/s)* and (c) Oil-in-water and water-in-oil Dispersions *(U_{ws}=1.0 m/s, U_{os}=0.8 m/s)*.

4. CONCLUSIONS

In this study a new set of oil-water flow experimental data were collected in a horizontal 2.62-i.d. 12-m-long horizontal glass pipe. Pressure gradient and holdup measurements and flow pattern characterization have been used for the analysis of the drag reduction phenomenon. The detected lower mixture pressure gradient with respect to the single-phase water pressure gradient at the same mixture velocity confirmed the occurrence of the phenomenon in the dispersed flows studied. Mixture friction factor and the effective mixture viscosity were determined from the measured pressure gradients by using the homogeneous no-slip model assumption. The values of mixture friction factor and effective mixture viscosity found to be lower than the respective values of single-phase water flow at mixture velocity also indicate the occurrence of the drag reduction phenomenon and, in addition, suggest that it is stronger at low oil fractions.

The oil holdup measured by the quick-closing-valves technique has been compared with the oil holdup (oil cut) predicted by the homogeneous model. It should be pointed out that in the experiments the mixture Reynolds number ranged from 30000 to 120000. Quite surprisingly, the comparison showed that the no-slip model overestimated by 15% the experimental oil holdup for the three oil-in-water dispersed flow patterns observed: Oil-in-water Homogeneous Dispersion (**o/w H**), Oil-in-water Non-homogeneous Dispersion (**o/w NH**) and Oil-in-water and Water-in-oil Dispersions (**Do/w & Dw/o**). This result indicates that the oil is the faster flowing phase. Therefore, the studied horizontal oil-in-water dispersed flows presented slip ratio and the homogeneous no-slip model assumption may not be a reliable route for the accurate two-phase pressure gradient prediction.

The capacitive wire-mesh sensor was used for the first time to characterize and for holdup measurements in viscous oil-water flow. The comparison between the oil holdup obtained by the quick-closing-valves technique and the oil holdup obtained by the wire-mesh sensor presented an accuracy of 15% and average relative error of 13.6 %, which is considered a quite good result. The wire-mesh sensor provided oil holdup distributions integrated over different domains and cross-sectional images of the phases distribution. In general, those results showed the presence of a higher amount of water near to the pipe wall in all the dispersed flow patterns observed. The detected water film seems to be surrounding the mixture of oil in water and acting as a lubricant, which may explain the slip ratio and the physics behind the drag reduction phenomenon.

5. ACKNOWLEDGEMENTS

The authors are grateful to CAPES (Coordenação de Aperfeiçoamento de Pessoal de Nível Superior) and FAPESP (Fundação de Amparo à Pesquisa do Estado de São Paulo, proc. 2008/06922-9) for the financial support given to this research and also to Dresden-Rossendorf Research Center (Germany) for the contribution in the experimental work. Iara Rodriguez would like to thank Dresden-Rossendorf Research Center (Germany) for providing financial support for her student internship.

6. REFERENCES

Angeli, P. and Hewitt, G.F., 1998, “Pressure gradient in horizontal liquid-liquid flows”, International Journal of Multiphase Flow, Vol. 24, pp .1183-1203.

Da Silva, M. J., Schleicher, E. and Hampel, U., 2007, “Capacitance wire-mesh sensor for fast measurement of phase fraction distributions”, Measurement Science and Technology, Vol. 18, pp.2245-2251.

de Castro, M.S., Rodriguez, I.H. and Rodriguez, O.M.H., 2009, “A prospective model for drag reduction phenomenon in oil-water dispersed pipe flow”, 20th International Congress of Mechanical Engineering, Gramado, RS, Brazil, November 15-20 (submitted).

Guet, S., Rodriguez, O.M.H., Oliemans, R.V.A. and Brauner, N., 2006. “An inverse dispersed multiphase flow model for liquid production rate”. International Journal of Multiphase Flow, Vol. 32, pp. 553-567.

Ioannou, K. et al., 2005, “Phase inversion in dispersed liquid- liquid flows”, Experimental Thermal and Fluid Science, Vol. 29, pp. 331-339.

Hu, B. and Angeli, P., 2006, “Phase Inversion and associated phenomena en oil-water vertical pipeline flow”, The Canadian Journal of Chemical Engineering, Vol. 84, pp. 94-107.

Lovick, J. and Angeli, P., 2004, “Experimental studies on the dual continuous flow pattern in oil-water flows”, International Journal of Multiphase Flow, Vol. 30, pp. 139-157.

Lum, J.Y.L. et al., 2006, “Upward and downward inclination oil-water flows”, International Journal of Multiphase Flow, Vol. 32, pp. 413-435.

Pal, R., 1993, “Pipeline Flow of Unstable and Surfactant Stabilized Emulsions”, AIChE Journal., Vol. 39, n.11, pp. 1754-1764.

Pal, R., 2007, “Mechanism of turbulent Drag Reduction in emulsions and bubbly suspensions”, Industrial & Engineering Chemistry Research, Vol. 46, pp. 618-622.

Prasser, H. M., Bottger, A. and Zschau. J., 1998, “A new electrode mesh tomograph for gas-liquid flows”, Flow Measurement and Instrumentation, Vol. 9, pp. 111-119.

McKeen, T. R. and Pugsley, T. S., 2002, “The influence of permittivity models on phantom images obtained from electrical capacitance tomography”, Measurement Science and Technology, Vol. 13, pp. 1822-1830.

Rodriguez, O.M.H., 2005, “Inversion of multiphase flow models for multiphase well logging”, Fourth progress report, Vol. 1 - Experimental work, Shell International Exploration and Production B.V. Report, Rijswijk, The Netherlands, February 03.

Wallis, G.B., 1969, “One-Dimensional Two-Phase Flow”, MacGraw-Hill, New York

7. RESPONSIBILITY NOTICE

The authors are the only responsible for the printed material included in this paper.